Nanoscale Research Letters

NANO EXPRESS

Open Access

CrossMark

Structure Peculiarities of Micro- and Nanocrystalline Perovskite Ferrites La$_{1-x}$Sm$_x$FeO$_3$

O. B. Pavlovska[1], L. O. Vasylechko[1*], I. V. Lutsyuk[2], N. M. Koval[3], Ya A. Zhydachevskii[1,4] and A. Pieniążek[4]

Abstract

Micro- and nanocrystalline lanthanum-samarium ferrites La$_{1-x}$Sm$_x$FeO$_3$ with orthorhombic perovskite structure were obtained by using both solid state reactions (x = 0.2, 0.4, 0.6 and 0.8) and sol-gel synthesis (x = 0.5) techniques. Obtained structural parameters of both series of La$_{1-x}$Sm$_x$FeO$_3$ are in excellent agreement with the "pure" LaFeO$_3$ and SmFeO$_3$ compounds, thus proving formation of continuous solid solution in the LaFeO$_3$–SmFeO$_3$ system. Peculiarity of La$_{1-x}$Sm$_x$FeO$_3$ solid solution is divergence behaviour of unit cell dimensions with increasing x: systematic decrease of the a and c lattice parameters is accompanied with increasing b parameter. Such behaviour of the unit cell dimensions in La$_{1-x}$Sm$_x$FeO$_3$ series led to crossover of the a and c perovskite lattice parameters and formation of dimensionally tetragonal structure near x = 0.04. Linear decrease of the unit cell volume of La$_{1-x}$Sm$_x$FeO$_3$ with decreasing x according with the Vegard's rule indicate absence of short-range ordering of R-cations in the LaFeO$_3$–SmFeO$_3$ system.

Keywords: Mixed rare earth ferrites, Perovskites, Crystal structure, Solid solution, Lattice crossover

Background

The interest in the rare earth ferrites RFeO$_3$ (R = rare earths) is stimulated by their unique properties, such as high electrical conductivity, specific magnetic properties including spin reorientation phenomena, as well as significant electrochemical and catalytic activity. RFeO$_3$-based materials are used as electrode materials in solid oxide fuel cells [1, 2], as membranes for gases separation, sensory materials and catalysts [3–6], and as magnetic and multiferroic materials [7–10].

Among RFeO$_3$ compounds, lanthanum and samarium orthoferrites are two of the most studied materials because of combination of several intrigue properties [10–13]. At the ambient conditions, both LaFeO$_3$ and SmFeO$_3$ display the orthorhombic perovskite structure isotypic with GdFeO$_3$ [14, 15]. In situ high-resolution X-ray synchrotron and neutron powder diffraction examination revealed no structural changes in SmFeO$_3$ in the temperature range of 300–1173 K [16], whereas LaFeO$_3$ undergoes the first-order orthorhombic-to-rhombohedral structural phase transition at 1253–1260 K [17–19]. Lattice expansion of LaFeO$_3$ and SmFeO$_3$ shows non-linear and strongly anisotropic thermal behaviour: in both compounds relative expansion in b-direction is much lower than in a- and c-directions [16, 18–20]. As a result, lattice parameter crossovers occur in LaFeO$_3$ at 750–950 K [18–20]. Subtle anomalies in the lattice expansion detected in LaFeO$_3$ and SmFeO$_3$ are associated with antiferromagnetic—to paramagnetic phase transition occurred in these compounds at 735 and 670 K, respectively [11, 12, 16, 21]. In LaFeO$_3$, such anomalies are reflected in non-linear lattice expansion across the magnetic phase transition at the Néel temperature 735 K [18] and in the step of dilatometric thermal expansion coefficient at 723 ± 50 K. In SmFeO$_3$, the b parameter exhibits a small anomalous kink around 670 K that is indicative for magnetoelastic coupling at the magnetic ordering temperature T_N [16]. Similar sign of magnetoelastic coupling was recently detected in the mixed ferrite system SmFeO$_3$–PrFeO$_3$, in which subtle maxima at the thermal expansion curves were observed in Sm$_{0.5}$Pr$_{0.5}$FeO$_3$ at around 670 K [22].

* Correspondence: crystal-lov@polynet.lviv.ua
[1]Semiconductor Electronics Department of Lviv Polytechnic National University, 12 Bandera Street, 79013 Lviv, Ukraine
Full list of author information is available at the end of the article

Pavlovska *et al. Nanoscale Research Letters* (2017) 12:153

Page 2 of 6

The aim of the present work is synthesis of phase pure micro- and nanocrystalline powders of lanthanum-samarium orthoferrites $La_{1-x}Sm_xFeO_3$ and their detailed structural investigation in whole concentration range.

Methods

Micro- and nanocrystalline samples of the mixed lanthanum-samarium ferrites were prepared by two different experimental routes. Samples with nominal compositions $La_{1-x}Sm_xFeO_3$ ($x = 0.2, 0.4, 0.6$ and 0.8) were obtained by solid state reactions technique. Precursor oxides La_2O_3, Sm_2O_3 and Fe_2O_3 were ball-milled in ethanol for 5 h, dried, pressed into pellets and annealed in air at 1473 K for 40 h with one intermediate regrinding. The synthesis of $La_{1-x}Sm_xFeO_3$ can be presented by following reaction scheme:

$$(1-x)La_2O_3 + xSm_2O_3 + Fe_2O_3 \rightarrow 2La_{1-x}Sm_xFeO_3$$
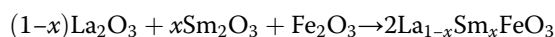
For a preparation of nanocrystalline powders of nominal composition, $La_{0.5}Sm_{0.5}FeO_3$ sol-gel citrate method was used. Crystalline salts $La(NO_3)_3 \cdot 6H_2O$ (99.99%, Alfa Aesar), $Sm(NO_3)_3 \cdot 6H_2O$ (ACS, Alfa Aesar) and $Fe(NO_3)_3 \cdot 9H_2O$ (ACS, Alfa Aesar) and citric acid (CC) were dissolved in water and mixed in the molar ratio of $n(La^{3+}){:}n(Sm^{2+}){:}n(Fe^{3+}){:}n(CC) = 1{:}0.5{:}0.5{:}4$ according to the nominal composition of the sample. Prepared solution was gelled at ~90 °C and heat treated at 1073 K for 2 h. After X-ray diffraction (XRD) examination, the part of the powder was additionally annealed at 1173 K for 2 h and then at 1473 K for 4 h. Thus three $La_{0.5}Sm_{0.5}FeO_3$ specimens, synthesized at different conditions, were obtained.

X-ray phase and structural characterization of the samples were performed by using Huber imaging plate Guinier camera G670 (Cu $K_{\alpha 1}$ radiation, $\lambda = 1.54056$ Å). Spot-check examination of the cationic composition was performed by energy dispersive X-ray fluorescence (EDXRF) analysis by using XRF Analyzer Expert 3L. Based on the experimental powder diffraction data, the unit cell dimensions and positional and displacement parameters of atoms in the $La_{1-x}Sm_xFeO_3$ structures were derived by full profile Rietveld refinement technique using software package WinCSD [23]. This programme package was also used for the evaluation of microstructural parameters of $La_{0.5}Sm_{0.5}FeO_3$ powders from angular dependence of the Bragg's maxima broadening. Average grain size, D_{ave} and microstrains $<\varepsilon> = <\Delta d>/d$ were derived both by full profile Rietveld refinement and by using Williamson-Hall analysis, which allows to separate the effect of size and strain broadening due to their different dependence on the scattering angle. In both cases, LaB_6 external standard was used for the correction of instrumental broadening. The morphology of sol-gel derived $La_{0.5}Sm_{0.5}FeO_3$ samples synthesized at different conditions was investigated by means of Hitachi SU-70 scanning electron microscope.
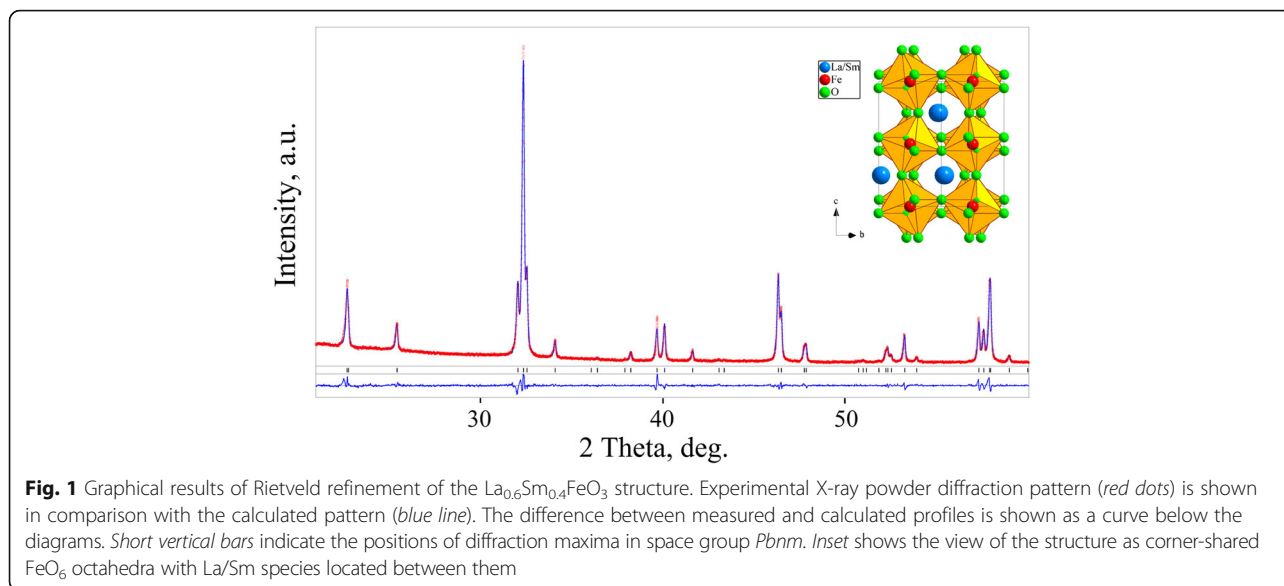
Results and Discussion

X-ray phase and structural analysis revealed that all $La_{1-x}Sm_xFeO_3$ samples synthesized by solid state method at 1473 K for 40 h adopt orthorhombic perovskite structure isotypic with $GdFeO_3$. No additional crystalline phases were found. Full profile Rietveld refinement, performed in space group *Pbnm*, shows excellent agreement between experimental and calculated diffraction patterns (Fig. 1) thus proving phase purity and crystal structure of the samples.

X-ray powder diffraction examination of sol-gel derived $La_{0.5}Sm_{0.5}FeO_3$ sample shows that even short-term heat treatment of the dried xerogel at 1073 K for 2 h led to formation of pure perovskite structure, without any traces of precursor components or other parasitic phases (Fig. 2). Substantial broadening of the diffraction maxima observed at the XRD pattern of $La_{0.5}Sm_{0.5}FeO_3@1073$ sample clearly indicates the nanoscale particle size of the as-obtained product.

Indeed, evaluation of microstructural parameters of the $La_{0.5}Sm_{0.5}FeO_3@1073$ sample from the analysis of the XRD profile broadening by full profile Rietveld technique lead to the average grain size $D_{ave} = 78$ nm and microstrains $<\varepsilon> = <\Delta d>/d = 0.17\%$. Additional heat treatment of the sample at 1173 and 1473 K does not affects on the phase composition and crystal structure parameters of the sample; the main changes occurs in the microstructural parameters, as it is evidenced from the significant narrowing of the Bragg's maxima, especially pronounced in $La_{0.5}Sm_{0.5}FeO_3@1473$ sample (Fig. 2). Evolution of the average grain sizes and microstrains in $La_{0.5}Sm_{0.5}FeO_3$ specimens vs synthesis temperature (Fig. 2, inset) clearly shows systematic increase of the average grain sizes, D_{ave}, accompanied with simultaneous reducing of the lattice strains. The D_{ave} values increases weakly from 78 to 103 nm after additional annealing at 1173 K for 2 h, whereas further heat treatment of the sample at 1473 K for 4 h lead to the drastic increase of the crystallite size up to >2000 nm. Similar evolution of the microstructural parameters of $La_{0.5}Sm_{0.5}FeO_3$ was obtained from the Williamson-Hall analysis (Fig 3). No obvious selective *hkl*-dependent peak broadening was observed for the samples heat treated at different temperatures.

Scanning electronic microscopy of the pristine $La_{0.5}Sm_{0.5}FeO_3$, obtained at 1073 K, revealed sheets-like morphology of the powder consisting of the particles of irregular form with linear dimensions 200–500 nm (Fig. 4a). Taking into account that average grain size of $La_{0.5}Sm_{0.5}FeO_3@1073$ sample derived from XRD data is 51–73 nm, it is evident that the particles observed at SEM picture of the sample

Pavlovska *et al. Nanoscale Research Letters* (2017) 12:153

Page 3 of 6

Fig. 1 Graphical results of Rietveld refinement of the $La_{0.6}Sm_{0.4}FeO_3$ structure. Experimental X-ray powder diffraction pattern (*red dots*) is shown in comparison with the calculated pattern (*blue line*). The difference between measured and calculated profiles is shown as a curve below the diagrams. *Short vertical bars* indicate the positions of diffraction maxima in space group *Pbnm. Inset* shows the view of the structure as corner-shared FeO_6 octahedra with La/Sm species located between them
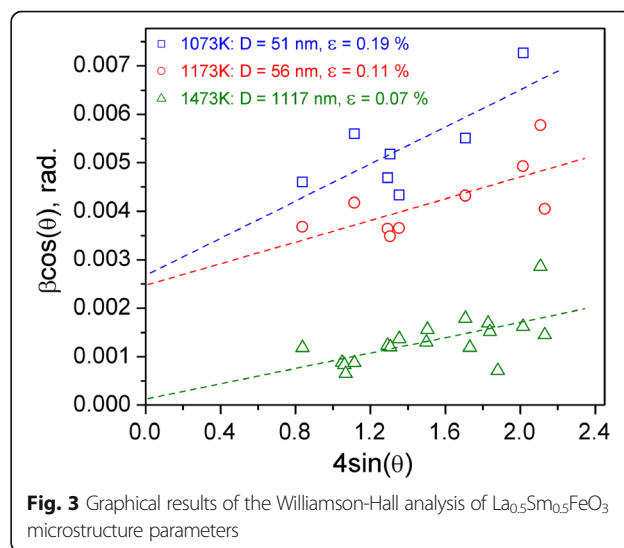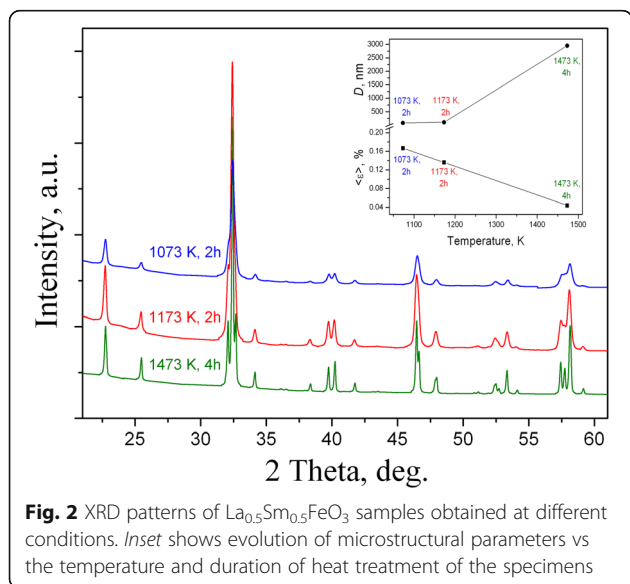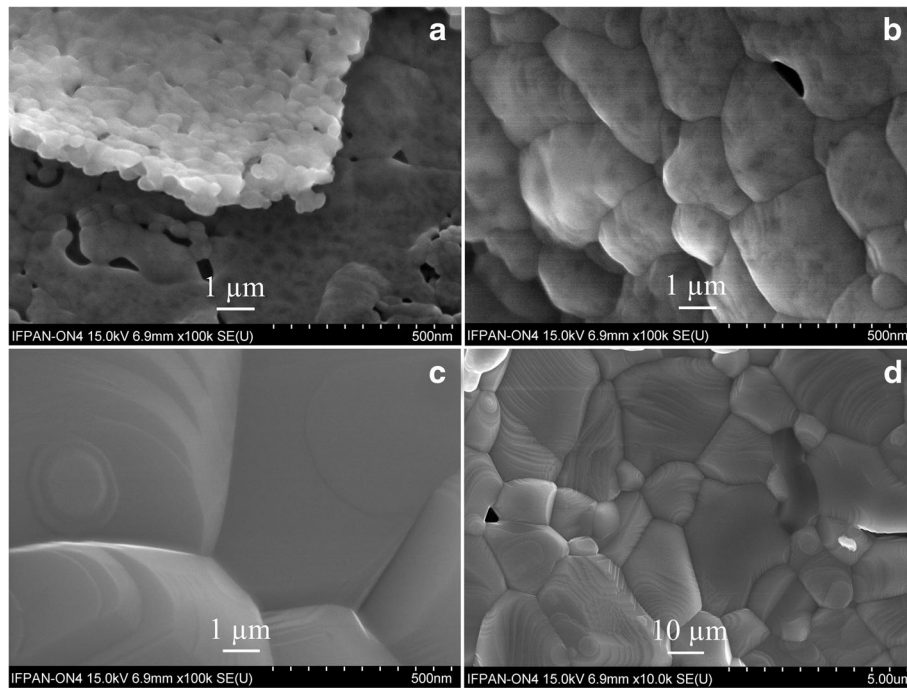
consist of several smaller crystallites. SEM examination also confirms the temperature evolution of microstructural parameters of $La_{0.5}Sm_{0.5}FeO_3$, derived from the X-ray powder diffraction data. As it is evidenced from Fig. 4b, additional heat treatment of the $La_{0.5}Sm_{0.5}FeO_3$ sample at 1173 K for 2 h leads to the particle agglomeration and formation of 1–5 μm agglomerates, consisting of several submicron particles. Finally, further heat treatment of the sample at 1473 K for 4 h lead to coalescence of small grains and particles and formation of 10–50 μm crystallites with clear signs of the facet growth (Fig. 4c, d).

Refined values of unit cell dimensions and positional and displacement parameters of atoms for sol-gel-derived $La_{0.5}Sm_{0.5}FeO_3$ samples, heat treated at 1073 and 1473 K,

as well as the $La_{1-x}Sm_xFeO_3$ specimens with $x = 0.2$, 0.4, 0.6 and 0.8, obtained by traditional ceramic technology are presented in Table 1.

Structural parameters of the mixed ferrites $La_{1-x}Sm_xFeO_3$ synthesized by different experimental techniques agree well with the parent $LaFeO_3$ and $SmFeO_3$ compounds [14, 15], as well as with the lattice parameters for Sm-doped $LaFeO_3$ recently reported [24]. An analysis of the concentration dependence of unit cell dimensions in $La_{1-x}Sm_xFeO_3$ series clearly proves the formation of continuous solid solution in the $LaFeO_3$–$SmFeO_3$ pseudo-binary system. The lattice parameters of $La_{1-x}Sm_xFeO_3$ change systematically between $LaFeO_3$ and $SmFeO_3$ showing divergence behaviour with increasing x: gradual decrease of the a- and c-parameters is accompanied with detectable increasing b parameter (Fig. 5).

Fig. 2 XRD patterns of $La_{0.5}Sm_{0.5}FeO_3$ samples obtained at different conditions. *Inset* shows evolution of microstructural parameters vs the temperature nand duration of heat treatment of the specimens

Fig. 3 Graphical results of the Williamson-Hall analysis of $La_{0.5}Sm_{0.5}FeO_3$ microstructure parameters

Pavlovska *et al. Nanoscale Research Letters* (2017) 12:153

Page 4 of 6
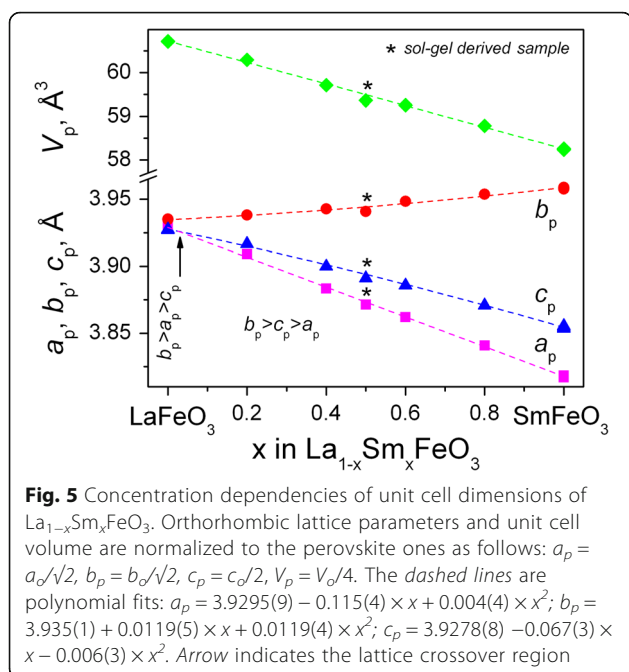

Fig. 4 SEM pictures of La$_{0.5}$Sm$_{0.5}$FeO$_3$ synthesized at 1073 K (**a**), 1173 K (**b**) and 1473 K (**c**, **d**)

Table 1 Lattice parameters, coordinates and displacement parameters of atoms in La$_{1-x}$Sm$_x$FeO$_3$ structures

Atoms, sites	Parameters, residuals	$x = 0.2$	$x = 0.4$	$x = 0.5^a$, 1073 K	$x = 0.5^a$, 1473 K	$x = 0.6$	$x = 0.8$
	a, Å	5.5284(8)	5.4921(5)	5.477(1)	5.4750(3)	5.4618(3)	5.4319(9)
	b, Å	5.5694(8)	5.5759(5)	5.565(1)	5.5731(3)	5.5839(3)	5.5914(9)
	c, Å	7.833(1)	7.8000(7)	7.782(2)	7.7825(4)	7.7717(4)	7.742(2)
	V, Å^3	241.19(8)	238.86(7)	237.2(2)	237.46(4)	237.02(4)	235.1(2)
La/Sm, 4c	x	−0.0087(3)	−0.0096(3)	−0.0032(10)	−0.0095(3)	−0.0105(2)	−0.0105(4)
	y	0.0354(2)	0.0432(1)	0.0421(2)	0.0448(1)	0.0481(1)	0.0523(2)
	z	1/4	1/4	1/4	1/4	1/4	1/4
	B_{iso}, Å^2	0.53(2)	0.51(2)	0.68(3)	0.54(2)	0.71(2)	0.71(3)
Fe, 4b	x	0	0	0	0	0	0
	y	1/2	1/2	1/2	1/2	1/2	1/2
	z	0	0	0	0	0	0
	B_{iso}, Å^2	1.15(4)	1.27(4)	1.38(6)	0.81(4)	0.99(3)	0.89(6)
O1, 4c	x	0.051(3)	0.080(2)	0.080(3)	0.0820(15)	0.0943(12)	0.087(2)
	y	0.5028(13)	0.4703(14)	0.466(2)	0.4764(13	0.4632(11)	0.468(2)
	z	1/4	1/4	1/4	1/4	1/4	1/4
	B_{iso}, Å^2	0.9(4)	2.4(3)	0.6(2)	2.4(2)	1.8(2)	0.5(3)
O2, 8d	x	−0.314(2)	−0.3047(12)	−0.315(2)	−0.2908(12)	−0.2837(9)	−0.3078(15)
	y	0.284(2)	0.2753(13)	0.274(2)	0.2865(12)	0.2863(9)	0.284(2)
	z	0.0392(15)	0.0475(9)	0.054(2)	0.0467(8)	0.0543(6)	0.0519(11)
	B_{iso}, Å^2	2.1(3)	1.5(2)	0.6(2)	1.5(2)	0.89(13)	0.6(3)
	R_I	0.071	0.056	0.104	0.046	0.053	0.089
	R_P	0.144	0.116	0.183	0.124	0.106	0.181

^{a}Synthesized by sol-gel method

Pavlovska *et al. Nanoscale Research Letters* (2017) 12:153

Page 5 of 6

Fig. 5 Concentration dependencies of unit cell dimensions of $La_{1-x}Sm_xFeO_3$. Orthorhombic lattice parameters and unit cell volume are normalized to the perovskite ones as follows: $a_p = a_o/\sqrt{2}$, $b_p = b_o/\sqrt{2}$, $c_p = c_o/2$, $V_p = V_o/4$. The *dashed lines* are polynomial fits: $a_p = 3.9295(9) - 0.115(4) \times x + 0.004(4) \times x^2$; $b_p = 3.935(1) + 0.0119(5) \times x + 0.0119(4) \times x^2$; $c_p = 3.9278(8) - 0.067(3) \times x - 0.006(3) \times x^2$. *Arrow* indicates the lattice crossover region

Such strongly anisotropic behaviour of the unit cell dimensions in $La_{1-x}Sm_xFeO_3$ series is explained by crystal structure peculiarities of the end members of the system—-LaFeO$_3$ and SmFeO$_3$. In spite of both compounds belong to the same GdFeO$_3$-type of crystal structure (space group *Pbnm*), they show different order of the perovskite cell parameters: $b_p > a_p > c_p$ for LaFeO$_3$ and $b_p > c_p > a_p$ for SmFeO$_3$. Consequently, a crossover of a_p- and c_p-parameters and formation of dimensionally tetragonal structure occurs in $La_{1-x}Sm_xFeO_3$ series near $x = 0.04$ (Fig. 4). Similar phenomena of the lattice parameters crossover were earlier observed in the mixed cobaltite-ferrites $PrCo_{1-x}Fe_xO_3$ and $NdCo_{1-x}Fe_xO_3$ [25, 26], as well as in the related rare earth aluminates and gallates $R_{1-x}R'_xAlO_3$ and $R_{1-x}R'_xGaO_3$ [27–30], in which the end members of the systems show different relations of the lattice parameters. In spite of the observed peculiarities lattice parameters behaviour, the unit cell volume in $La_{1-x}Sm_xFeO_3$ series decreases almost linearly with decreasing R-cation radii according to the Vegard's rule. This observation indicates statistical distribution of La and Sm species over positions of R-cations in $La_{1-x}Sm_xFeO_3$ perovskite lattice and absence of short-range ordering in LaFeO$_3$–SmFeO$_3$ system.

Conclusions

Single-phase micro- and nanocrystalline ferrites $La_{1-x}Sm_xFeO_3$ with orthorhombic perovskite structure were prepared by solid state reactions ($x = 0.2$, 0.4, 0.6 and 0.8) and sol-gel citrate route ($x = 0.5$). The lattice parameters and coordinates and displacement parameters of atoms in $La_{1-x}Sm_xFeO_3$ structures, as well as microstructural

parameters of $La_{0.5}Sm_{0.5}FeO_3$ nanopowders were derived from X-ray powder diffraction data by full profile Rietveld refinement technique. Obtained structural parameters of both solid state and sol-gel synthesized ferrites $La_{1-x}Sm_xFeO_3$ agree well and prove the formation of continuous solid solution in LaFeO$_3$–SmFeO$_3$ pseudo-binary system. Peculiarity of $La_{1-x}Sm_xFeO_3$ solid solution is divergence behaviour of unit cell dimensions with increasing samarium content and crossover of the a and c perovskite lattice parameters near $x = 0.04$. In comparison with a traditional energy- and time-consuming high-temperature ceramic technique, the low-temperature sol-gel citrate method is very promising tool for a synthesis of fine powders of the mixed perovskite oxide materials, free of contamination of parasitic phases.

Authors' Contributions
OP synthesized the samples by solid state reactions technique, contributed to the data evaluation and wrote the manuscript. LV performed the laboratory X-ray powder diffraction measurements, made the structural characterization of the samples and contributed to the manuscript writing. IL performed the sol-gel synthesis of the samples. NK performed the examination of the cationic composition of the samples by energy dispersive X-ray fluorescence (EDXRF) analysis. YZ and AP performed the scanning electron microscopy measurements and contributed to the manuscript writing. All authors read and approved the final manuscript.

Competing Interests
The authors declare that they have no competing interests.

Author details
[1]Semiconductor Electronics Department of Lviv Polytechnic National University, 12 Bandera Street, 79013 Lviv, Ukraine. [2]Department of Chemical Technology of Silicates of Lviv Polytechnic National University, 12 Bandera Street, 79013 Lviv, Ukraine. [3]Department of Ecological Safety and Nature Protection Activity of Lviv Polytechnic National University, 12 Bandera Street, 79013 Lviv, Ukraine. [4]Institute of Physics, Polish Academy of Sciences, Al. Lotników 32/46, 02-668 Warsaw, Poland.

References
1. Sun C, Hui R, Roller J (2010) Cathode materials for solid oxide fuel cells: a review. J Solid State Electrochem 14:1125–1144
2. Bukhari SM, Giorgi JB (2012) Chemically stable and coke resistant $Sm_{1-x}Ce_xFeO_{3-\delta}$ perovskites for low temperature solid oxide fuel cell anode applications. J Power Sources 198:51–58
3. Itagaki Y, Mori M, Hosoya Y, Aono H, Sadaoka Y (2007) O$_3$ and NO$_2$ sensing properties of $SmFe_{1-x}Co_xO_3$ perovskite oxides. Sens Actuator B 122:315–320
4. Goldwasser MR, Rivas ME, Lugo ML, Pietri E, Perez-Zurita J, Cubeiro ML et al (2005) Combined methane reforming in presence of CO$_2$ and O$_2$ over $LaFe_{1-x}Co_xO_3$ mixed-oxide perovskites as catalysts precursors. Catal Today 107–108:106–113
5. Wang Y, Yang X, Lu L, Wang X (2006) Experimental study on preparation of LaMO$_3$ (M = Fe, Co, Ni) nanocrystals and their catalytic activity. Thermochim Acta 443:225–230
6. Ding J, Lü X, Shu H, Xie J, Zhang H (2010) Microwave-assisted synthesis of perovskite ReFeO$_3$ (Re: La, Sm, Eu, Gd) photocatalyst. Mater Sci Eng B 171: 31–34

Pavlovska *et al. Nanoscale Research Letters* (2017) 12:153

Page 6 of 6

7. Tsymbal L, Bazaliy Y, Kakazei G, Vasiliev S (2010) Mechanisms of magnetic and temperature hysteresis in $ErFeO_3$ and $TmFeO_3$ single crystals. J Appl Phys 108:083906

8. Wang B, Zhao X, Wu A, Cao S, Xu J, Kalashnikova AM et al (2015) Single crystal growth and magnetic properties of $Sm_{0.7}Tb_{0.3}FeO_3$ orthoferrite single crystal. J Magn Magn Mater 379:192–195

9. Tokunaga Y, Furukawa N, Sakai H, Taguchi Y, Arima T, Tokura Y (2009) Composite domain walls in a multiferroic perovskite ferrite. Nature Mater 8:558–562

10. Acharya S, Mondal J, Ghosh S, Roy SK, Chakrabarti PK (2010) Multiferroic behavior of lanthanum orthoferrite ($LaFeO_3$). Mater Lett 64:415–418

11. Gorodetsky G, Levinson L (1969) Spin reorientation in $SmFeO_3$. Solid State Commun 7:67–70

12. Lee J, Jeong Y, Park J, Oak M, Jang H, Son J et al (2011) Spin-canting-induced improper ferroelectricity and spontaneous magnetization reversal in $SmFeO_3$. Phys Rev Letters 107:117201

13. Huang S, Shi L, Tian Z, Yuan S, Wang L, Gong G et al (2015) High-temperature colossal dielectric response in $RFeO_3$ (R = La, Pr and Sm) ceramics. Ceram Int 41:691–698

14. Marezio M, Remeika J, Dernier P (1970) The crystal chemistry of the rare earth orthoferrites. Acta Cryst B 26:2008–2022

15. Berenov A, Angeles E, Rossiny J, Raj E, Kilner J, Atkinson A (2008) Structure and transport in rare-earth ferrates. Solid State Ionics 179:1090–1093

16. Kuo C, Drees Y, Fernández-Díaz M, Zhao L, Vasylechko L, Sheptyakov D et al (2014) k = 0 magnetic structure and absence of ferroelectricity in $SmFeO_3$. Phys Rev Lett 113:217203

17. Geller S, Raccah P (1970) Phase transitions in perovskite-like compounds of the rare earths. Phys Rev B 2:1167–1172

18. Selbach SM, Tolchard JR, Fossdal A, Grande T (2012) Non-linear thermal evolution of the crystal structure and phase transitions of $LaFeO_3$ investigated by high temperature X-ray diffraction. J Solid State Chem 196:249–254

19. Fossdal A, Menon M, Wærnhus I, Wiik K, Einarsrud M-AN, Grande T (2004) Crystal structure and thermal expansion of $La_{1-x}Sr_xFeO_{3-\delta}$ materials. J Am Ceram Soc 87:1952–1958

20. Dixon CAL, Kavanagh CM, Knight KS, Kockelmann W, Morrison FD, Lightfoot P (2015) Thermal evolution of the crystal structure of the orthorhombic perovskite $LaFeO_3$. J Solid State Chem 230:337–342

21. Stølen S, Grønvold F, Brinks H, Atake T, Mori H (1998) Heat capacity and thermodynamic properties of $LaFeO_3$ and $LaCoO_3$ from T = 13 K to T = 1000 K. J Chem Thermodyn 30:365–377

22. Pavlovska O, Vasylechko L, Buryy O (2016) Thermal behaviour of $Sm_{0.5}R_{0.5}FeO_3$ (R = Pr, Nd) probed by high-resolution X-ray synchrotron powder diffraction. Nanoscale Res Lett 11:107

23. Akselrud L, Grin Y (2014) WinCSD: software package for crystallographic calculations (Version 4). J Appl Cryst 47:803–805

24. Swatsitang E, Karaphun A, Phokha S, Hunpratub S, Putjuso T (2016) Investigation of structural, morphological, optical, and magnetic properties of Sm-doped $LaFeO_3$ nanopowders prepared by sol–gel method. J Sol-Gel Sci Technol 80:1–10

25. Pekinchak O, Vasylechko L, Lutsyuk I, Vakhula Y, Prots Y, Carrillo-Cabrera W (2016) Sol-gel prepared nanoparticles of new mixed praseodymium cobaltites-ferrites. Nanoscale Res Lett 11:75

26. Pekinchak O, Vasylechko L, Berezovets V, Prots Y (2015) Structural behaviour of $EuCoO_3$ and mixed cobaltites-ferrites $EuCo_{1-x}Fe_xO_3$. Solid State Phenom 230:31–38

27. Vasylechko L, Senyshyn A, Bismayer U (2009) Perovskite-type aluminates and gallates. In: Gschneidner KA Jr, Bünzli J-CG, Pecharsky VK (eds) Handbook on the physics and chemistry of rare earths, vol 39. North-Holland, Netherlands, pp 113–295

28. Ohon N, Vasylechko L, Prots Y, Schmidt M (2014) Phase and structural behaviour of $SmAlO_3$–$RAlO_3$ (R = Eu, Gd) systems. Mater Res Bull 50:509–513

29. Vasylechko L, Berkowski M, Matkovskii A, Piekarczyk W, Savytskii D (2000) Structure peculiarities of the $La_{1-x}Nd_xGaO_3$ solid solutions. J Alloys Compd 300–301:471–474

30. Berkowski M, Fink-Finowicki J, Byszewski P, Diduszko R, Kowalska E, Aleksijko R et al (2001) Czochralski growth and structural investigations of $La_{1-x}Pr_xGaO_3$ solid solution single crystals. J Crystal Growth 222:194–201